
영상유체보존식과 함수전개법에 의한 심장영상의 광류

김진우*

Optical flow of heart images by image-flow conservation equation and functional expansion

Jin-Woo Kim*

요약

기존의 광류 (Optical flow)는 국소적 처리를 시작점으로 하는 bottom-up수법에 의해서 구하였다. 이에 반해, 본 논문은 영상유체보존식과 함수 전개법에 의해 영상 전체의 움직임을 차수가 낮은 모드로부터 순차적으로 전개하는 bottom-down수법을 새로운 수법으로 제안한다. 의료 영상에 있어서 명도는 움직임이 있어도 불변으로 유지하려는 경우가 많다. 그러나 이 같은 영상계열에서의 움직임은 좌표 변환에 의해서 대응된다. 본 수법의 경우 광류는 선형모멘트방정식의 함수에 관한 도함수를 이용하는 투영법에 의해서 반복계산으로 구하여진다. 본 논문에서는 심장의 영상계열을 이용하여 기존의 Horn and Schunck기법, Standard multigrid기법과 본 수법의 알고리즘을 비교 평가하여 유효성을 나타낸다.

ABSTRACT

The displacement field (Optical flow) has been calculated by bottom-up approaches based on local processing. In contrast with them, in this paper, a top-down approach based on expanding in turn from the lowest order mode the whole motion in an image pair of sequential images is proposed.

The intensity of medical images usually represents a quantity which is conserved during the motion. Hence sequential images are ideally related by a coordinate transformation. The displacement field can be determined from the generalized moments of the two images. The equations which transform arbitrary generalized moments from a source image to a target image are expressed as a function of the displacement field. The apparent displacement field is then computed iteratively by a projection method which utilizes the functional derivatives of the linearized moment equations. This method is demonstrated using a pair of sequential heart images.

For comparative evaluation, we applied Horn and Schunck's method, a standard multigrid method, and our proposed algorithm to sequential image.

키워드

Motion image, Optical flow, Medical image, Moment transform

I. INTRODUCTION

Two classes of techniques which have been used for motion measurement are pattern matching and gradient

methods. pattern matching methods require identification of a pattern in sequential images. The pattern can be an edge or other structure or simply a region in one image which is used as a kernel for searching a second image. Pattern matching

methods can fail if a pattern is ambiguous (e.g. repeated) or if the motion severely distorts its shape. Gradient methods utilize the differential brightness constancy equation to compute small displacements in the direction of brightness gradients in each image[1]. The remainder of the motion field is then determined by regularization, which is the application of smoothness constraints. Gradient methods have the drawback that the displacement must be small compared to the scale length of the intensity gradients in the image. The regularization process arbitrarily imposes smoothness in the motion, and therefore can distort the real variations in displacement. Most optical flow calculations do not allow explicitly for any sources of intensity. A recent attempt to include sources was made by Prince and McVeigh [2], but their technique used a specific model for the source term and required an a priori estimate of the motion.

A different method of motion computation was recently developed which is based on brightness constancy and the resulting relationship between weighted integrals of sequential images. The linearized integral transformation equations are taken as constraints, and the estimated motion and brightness changes can be computed by the method of convex projections [3-5]. By suitable choice of weighting functions, the motion estimate is built up at varying scale lengths by Fourier components. This differs from multiresolution methods [6-8] in which the image intensity rather than the motion itself is separated into different scale lengths. However, this technique still contained an arbitrary parameter, analogous to the arbitrary weights of regularization formulas used with gradient-based methods. In this paper, we demonstrate the effectiveness of our proposed method by comparing with conventional methods including Horn and Schunck's method, a standard multigrad optical flow algorithm.

II. METHODS

The transformation which relates two images $\rho_1(r)$ and $\rho_2(r)$ in a time sequence consists of two part : (1) a

displacement field $s(r)$ and (2) intensity sources $\rho_s(r)$. Only two-dimensional images with $r = (x, y)$ are considered here, but generalization to three or more dimensions is straightforward. It is easy to see that a transformation relating two images is not unique. For example the transformation between any two images, even if related by a simple translation, can be represented purely by intensity sources equal to the difference between the two images. Therefore additional criteria are required in order to obtain a unique solution. Some physical insight into this problem is obtained by examining the temporal change in image intensity ρ due to motion and sources. One possibility is to model the image intensity as the local density of a fluid. The general fluid conservation law with sources is :

$$\frac{\partial \rho}{\partial t} + \nabla \cdot \rho u = \frac{\partial \rho_s}{\partial t} \quad (1)$$

where $u = \partial s / \partial t$. The convective derivative $d\rho/dt$ represents the change in intensity as seen by an observer moving with an image point and is given by :

$$\frac{d\rho}{dt} = \frac{\partial \rho}{\partial t} + u \cdot \nabla \rho = \frac{\partial \rho_s}{\partial t} - \rho \nabla \cdot u \quad (2)$$

In a finite time interval, the change in convected intensity is $D\rho = \delta\rho_s - \rho \nabla \cdot \delta s$. Note that a given convected intensity change $D\rho$ consists of two terms which can be added together in any combination. The optimal solution is assumed to be the one which minimizes the magnitudes of the terms $\delta\rho_s$ and $\rho \nabla \cdot \delta s$. Since each term contributes equally to the convective derivative, they are weighted equally. The squared norm is therefore taken to be the sum of the squared norms of each of these terms :

$$\begin{aligned} \|v\|^2 &= \int dr p(r) (|\rho \nabla \cdot \delta s|^2 + |\delta \rho_s|^2) \quad (3) \\ &= \|\rho \nabla \cdot \delta s\|^2 + \|\delta \rho_s\|^2 \end{aligned}$$

where $v = (\delta s \cdot \delta \rho_s)$ and $p(r)$ is a non-negative weighting function which will be determined below. To be precise, this a true norm for the pair $(\rho \nabla \cdot \delta s, \delta \rho_s)$ rather than for v itself, but for simplicity the notation $\|v\|^2$ is used. The importance of the metric factor $p(r)$ is that it can be a function of the image intensity $\rho(r)$. If this factor is taken to be $p(r) = 1/\rho$, then the norm is given by :

$$\|v\|^2 = \int dr \rho \left(|\nabla \cdot \delta s|^2 - \left| \frac{\delta \rho_s}{\rho} \right|^2 \right) \quad (4)$$

Note that in this case the square norm of the convective derivative $D\rho$ is given by :

$$\begin{aligned} \int dr \rho \left(\left| \frac{\delta \rho_s}{\rho} - \nabla \cdot \delta s \right|^2 \right) = \\ \int dr \left(\frac{1}{\rho} |\delta \rho_s|^2 - 2(\nabla \cdot \delta s)(\delta \rho_s) + \rho |\nabla \cdot \delta s|^2 \right) \end{aligned} \quad (5)$$

Hence the cross-correlation between the two terms is independent of the local image intensity. In other words, the interference is spread out over the image rather than being concentrated in regions of high (or low) intensity. This means that there is no tendency for the motion to align itself with intensity gradients in the images.

Note that the norm in Eq.(4) is zero for incompressible motion without sources. For this type of motion it is appropriate simply to minimize the norm of the displacement field. A modified norm can combine compressible and incompressible motions as follows :

$$\|v\|^2 = \lim_{\alpha \rightarrow 0} \int dr \rho \left(\alpha |\delta s|^2 + |\nabla \cdot \delta s|^2 + \left| \frac{\delta \rho_s}{\rho} \right|^2 \right) \quad (6)$$

with $\alpha \geq 0$. The term containing α is only significant when the other terms are zero.

This norm is optimal in the following sense. The image intensity is treated as a fluid density. As a small region (fluid

element) moves from one image to the next, its intensity (fluid density) can change due to expansion or contraction, or due to sources. This norm minimizes the changes in image intensity from both of these effect. Notice that there is no cost associated with shear or rotation, since such motions do not change the image intensity along a trajectory. Hence smoothness of motion is not arbitrarily imposed. Of course, the above norm may not be optimal if additional a priori information is available regarding the physical characteristics of the images.

It has been assumed that the image intensity represents a physical quantity which obeys a kind of conservation law with sources. The model may be more appropriate for some specific function of intensity. For example, X-ray film intensity ideally represents a uniform incident intensity which is reduced exponentially by some absorbing material between the source and the image. Since the optical flow represents motion of this absorbing material, the logarithm of intensity is a better approximation to a conserved quantity, and should be represented by ρ . For scene analysis, the image typically represents light reflected or scattered from surfaces moving under nearly constant illumination. If absorption is negligible, then small variations in position or orientation modify the direction of reflection and the angular distribution of scattered light without changing the integrated intensity, so that the reflected light acts as a conserved quantity. Absorption can be represented as a negative source. Hence it is appropriate to let ρ be the image intensity in the equations above.

The integrand in Eq.(6) is zero in regions of zero intensity (actually the source term is undefined). Therefore the computed motion in dark regions of the image is arbitrary. This not a drawback in terms of visualization, but may be undesirable physically if material is present in these regions but not imaged. If interpolation of motion is desired in these dark regions, or if sources (such as noise) are present in these regions, then either the image intensity should be made nonzero everywhere or a different metric factor $p(r)$ should be used.

Eq(6) can be used for regularization of optical flow as computed by standard gradient-based methods. Such

methods are limited to small displacements, however, by the linear approximation $\rho(r + s) \approx \rho(r) + s \cdot \nabla \rho(r)$. For the results below, the motion is computed by solving a series of integral constraint Eq. (3)~(5). The constraints are of the form :

$$\int dr_2 g_n(r_2) \rho_2(r_2) = \int dr_1 g_n(r_1 + s) [\rho_1(r_1) + \rho_s(r_1)] \quad (7)$$

where $\rho_1(r_1)$ and $\rho_2(r_2)$ are the image intensities and $g_n(r)$ is arbitrary weighting function. The motion is computed by iteratively projecting onto the solution space of each constraint equation.

III. EXPERIMENTAL RESULTS

For comparative evaluation, we applied Horn and Schunck's method, a standard multigrid method, and our proposed algorithm to sequential image. The comparison of the three methods are carried out mainly by evaluating the similarities between the original second image and an estimated second image which is generated using the original first image and the optical flow obtained by each method. Three evaluation criterions of accuracy factor, RMS error and correlation are adopted. These evaluation values are shown in (8), (9), and (10).

$$R = \frac{1}{\max(N_A, N_I)} \sum_{i=1}^{N_A} \frac{1}{1 + (\alpha d_i^2)} \quad (8)$$

where N_A and N_I represent the number of actual and ideal edge map point, α is a scaling constant, and d is the separation distance of an actual edge point normal to a line of ideal edge point.

$$\text{RMS error} = \sqrt{\frac{\sum_x \sum_y (I(x, y, t) - \hat{I}(x, y, t))^2}{M \times N}} \quad (9)$$

where $I(x, y, t)$ and $\hat{I}(x, y, t)$ are the actual and estimated images of size $M \times N$ at time t .

$$\text{Correlation} = \frac{\sum_x \sum_y (I(x, y, t) - \bar{I})(\hat{I}(x, y, t) - \bar{\hat{I}})}{\sqrt{\sum_x \sum_y (I(x, y, t) - \bar{I})^2} \sqrt{\sum_x \sum_y (\hat{I}(x, y, t) - \bar{\hat{I}})^2}} \quad (10)$$

where $\bar{I} = [\sum_x \sum_y I(x, y, t)] / M \cdot N$ and $\bar{\hat{I}} = [\sum_x \sum_y \hat{I}(x, y, t)] / M \cdot N$ while $I(x, y, t)$ are the actual and estimated image of size $M \times N$ at time t .

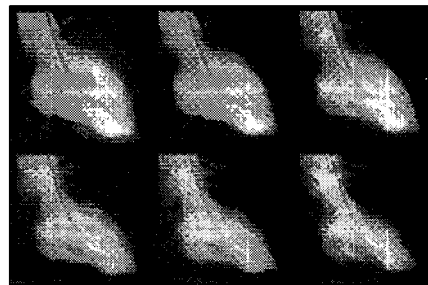
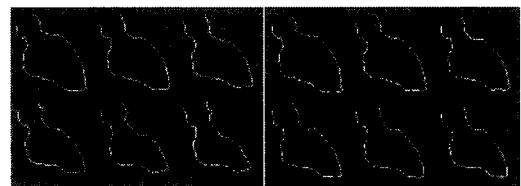
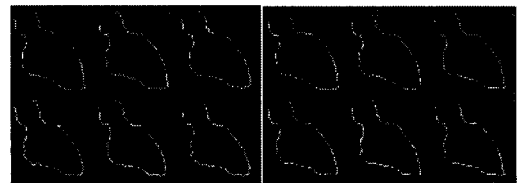


Fig. 1. Six images of a heart Sequence (128x128)



(a) original images

(b) using the proposed method



(c) using standard multigrid

(d) Horn & Schunck method

method

Fig. 2. Thinned edges of original and estimated heart images

This sequence (38 frames, 256x256) shows the pumping process of a heart. We choose 6 frames (No. 5 to No. 10) of the sequence and select their center parts (128x128) as working images (Fig. 1). The heart motion in these images is mainly a convergence motion. The movements of the

upper right and the lower-left parts are larger than the motion of other parts. To examine the effects of displacement sizes on the optical flows, the frame No. 5 is chosen as the first image and others are considered as the second image. We use the accuracy factor defined in (8), to investigate the edge location accuracy of heart in the estimated second images. To extract the edges of heart in the images first we binarized images are detected using Prewitt filter, and thinned to become one pixel width (Fig. 2).

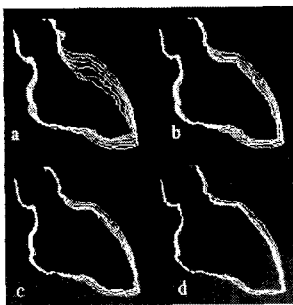
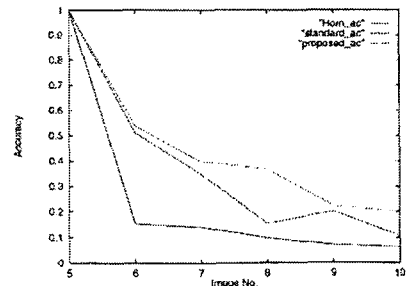


Fig. 3. Condensed images of Fig. 2

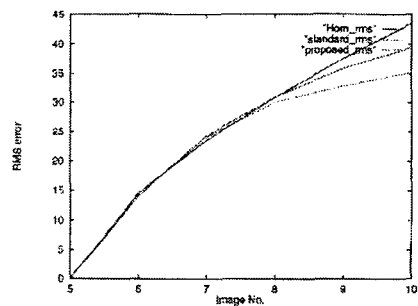
To become able to compare these results by eyes, their condensed form are shown in Fig. 3 which it shows the proposed algorithm is effective in the parts with large motion. Applying the results to Eq. (8), Fig. 4(a) is obtained which it shows the best results belong to proposed algorithm. The comparison of three methods using RMS error and correlation between the real and the estimated second images of heart sequence images are shown in Figures 4(b) and 4(c), respectively. According to these comparisons here also generally the better results belong to the proposed algorithm specially for image pairs which contains large displacements.

The estimated optical flows between image frames Nos. 5 and 10 using Horn and Schunck, standard multigrid, and proposed methods are shown in Fig. 5. Referring to this figure the difference among the estimated flows for three methods is the differences between the length of flows. The estimated images of image frame No. 4 obtained by applying the flows of Fig. 5 to the image frame No. 1 of heart sequence, together with the image frame No. 10 of this

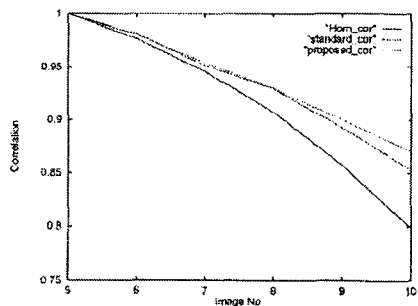
sequence are shown in Fig. 6.



(a) accuracy factor



(b) RMS error



(c) correlation

Fig. 4. Comparisons of the original and estimated second images using (a) accuracy factor, (b) RMS error, and (c) correlation

Fig. 7 shows the flow differences between the flows of Fig. 5. According to flow differences shown in Fig. 7 the most different flows are belong to the upper right and lower parts of heart which have the largest movement. This approves of the effectiveness of our method for large motions.

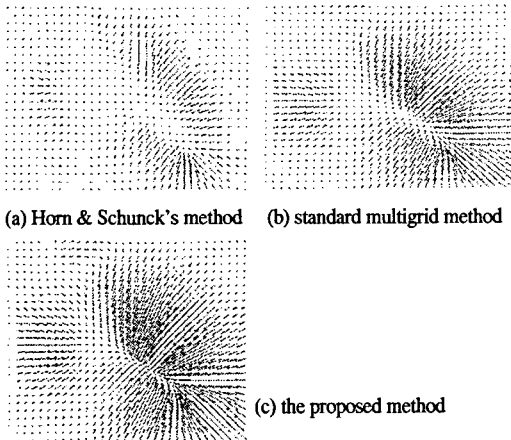


Fig. 5. The estimated flow between image frames Nos. 5 and 10 of heart sequence using three optical flow algorithm

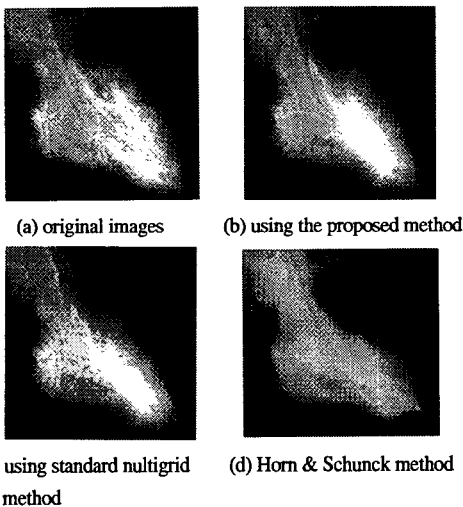


Fig. 6. The estimated and original images of image frame No. 10 of heart sequence using three optical flow algorithm

IV. CONCLUSIONS

The squared norm has been derived which minimizes contributions to change in convected intensity. The dominant terms in the squared norm represent divergent motion and independent sources. If both of these can be set to zero, then only the norm of the displacement is considered. This squared norm is proportional to the image

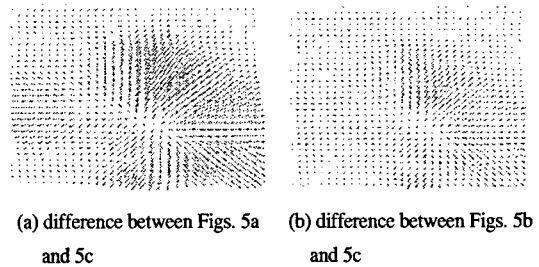


Fig. 7. The differences between flows estimated by our proposed algorithm and (a) Horn and Schunck, (b) standard multigrid algorithms

intensity. Having a brief and general view on the results it can be concluded that the proposed method having the ability of better flow estimation in comparison with Horn and Schunck's method and a standard multigrid method. As for heart sequence the correct flows are not known, we applied the resulted flows to the first image and estimated the second image, then compared the estimated second image to the real second image using accuracy factor of edges, RMS error and correlation factors. This heart sequences the best results belonged to the proposed algorithm. We can investigate the better flow estimation of the proposed algorithm by observing the estimated flows and image also. Applications for this method include the measurement of blood flow from MRI images, in which initially straight lines evolve according to the motion.

REFERENCES

- [1] B.K.P. Horn and B.G. Schunck, "Determining optical flow," *Artif. Intell.*, vol. 17, pp. 185-204, 1981.
- [2] J.L. Prince and E.R. McVeigh, "Motion estimation from tagged MR image sequences," *IEEE Trans. Med. Imag.*, vol. 11, no. 2, pp. 238-249, 1992.
- [3] L.M. Bregman, "Finding the common point of convex sets by the method of successive projection," *Dokl. Akad. Nauk SSSR*, vol. 162, no. 3, pp.487-490, 1965.
- [4] L.G. Gubin, B.T. Polyak, and E.V. Raik, "The method fo projections for finding the common point of convex sets," *U.S.S.R. Computational Math. Math. Phys.*, vol. 7, no. 6, pp. 1-24, 1967.
- [5] D.C. Youla and H. Webb, "Image restoration by the

- method of convex projections: part I-Theory," IEEE Trans. Med. Imag., vol. MI-I, pp. 81-94, 1982.
- [6] S.V. Fogel, "The estimation of velocity vector fields from time-varying image sequences," CVGIP: Image Understanding, vol. 53, no. 3, pp. 253-287, 1991.
- [7] W. Enkelmann, "Investigations of multigrid algorithms for the estimation of optical flow fields in image sequences," Comput. Vision Graphics Image Process., vol. 42, pp. 150-177, 1988.
- [8] R. Battiti, E. Amaldi, and C. Koch, "Computing optical flow across multiple scales: an adaptive course-to-fine strategy," Int. J. Comput. Vision, vol. 6, no. 2, pp. 133-145, 1991.

저자소개

김진우(Jin-Woo Kim)



1992년 명지대학교 전기공학과
(공학사)

1996년 일본 Fukui대학 전자공학과
(공학석사)

1999년 일본 Fukui대학 시스템설계공학(공학박사)

2000년~2003년 2월 한밭대학교 컴퓨터정보통신공학과
계약교수

2003년 3월~현재 경성대학교 멀티미디어통신공학과
조교수

※ 관심분야: (의료)영상신호처리, 컴퓨터비전, 객체추적,
생체인식 시스템